JOURNAL OF APPLIED ELECTROCHEMISTRY **27** (1997) 699–705

Electrodeposition of copper and nickel on InBi alloy electrodes

M. AZZAG, M. CHATELUT, O. VITTORI*

Laboratoire d'Electrochimie Analytique – LICAS, Université LYON I, Bât 308, ESCPE Lyon, 43 Bd du 11 Novembre 1918, 69622 Villeurbanne Cedex, France

Received 27 March 1996; revised 23 September 1996

Electrodeposition of copper and nickel was investigated on the 67–33 w/w InBi soft alloy, which has a low melting point (72 °C). The electrochemical behaviour of this alloy was found to be similar to that of pure indium in a Watt's type bath. Direct and pulsed current techniques were compared. For copper, a current density ranging from 500 to 1000 $A\,m^{-2}$ was found to be suitable to obtain regular and shiny deposits at 25 °C. For nickel, at 45 °C, the current density range used was 500 to 1250 $A\,m^{-2}$ to obtain good deposits, that were not affected by hydrogen evolution. Pulsed and direct currents were found to be equally efficient. The main interest of electrodeposition on InBi alloy was the ease of removal of the alloy by simple melting, and consequently to make electrodes of unusual shapes which are normally difficult to produce industrially. Only a small amount of InBi alloy remained in the inner part of the deposit.

1. Introduction

The major advantage of soft alloys is their low melting point. This allows the removal of the support by melting it at moderate temperature without damage to the deposit itself. This procedure is of interest to produce special devices, which are normally difficult or time consuming to obtain by mechanical processing.

To the authors knowledge, no study concerning copper and nickel electrodeposition on InBi alloys has been reported, and the electrochemical behaviour of bismuth and indium have received little attention. For bismuth, the anodic oxidation has been investigated in basic medium [1–3]. Other studies have concerned its passivation in HCl [4], and the competition between oxidation and dissolution in H_2SO_4 [5]. The effects of oxygen [6] or anions such as nitrate and thiocyanate [7–11] on oxide electrodissolution have also been studied.

Indium and indium–bismuth eutectic composition were studied in HCl medium [12]. It appears that chloride ions favour the electrodissolution of both In and Bi. Other work in perchloric [13, 14] and sulfuric acids [15–19] confirmed the kinetic effects of chloride ions.

In this paper we first describe the behaviour of indium, bismuth and the 66.66–33.33 w/w InBi alloy in sulfuric and boric acids. Then, for copper in sulfuric acid and nickel in a Watt's bath, we compare the performance of electrodeposition techniques using direct or pulsed currents.

2. Experimental details

A PJT 24–1 potentiostat coupled to a GSTP3 signal generator (Tacussel, France) and a LY1600 X–Y recorder (Linseis, Germany) were used for all experiments.

The reference was a saturated KCl calomel electrode. For studies concerning electrochemical behaviours in acidic solutions the auxiliary electrode was a platinum wire (Tacussel, France). For electrodeposition auxiliary electrode was either copper or nickel plate of a larger size compared to that of the working electrode. Indium, bismuth and indium–bismuth alloy electrodes were made with pure metals (99.9% Aldrich, USA). The alloy was made by melting and carefully mixing the appropriate masses of the two components. The density of the alloy was found to be 7.73 $g\,cm^{-3}$ The electrodes were designed as 5 mm diameter rods by moulding the molten metals. After slow cooling to room temperature the metal rod was polished with an abrasive CSi paper (15 μm) and rinsed with distilled water before experimentation. The moulds were prepared using silicon rubber, stable up to +230 °C (Roth. Sochiel, France), by embedding a 5 mm glass rod in the rubber during polymerization. After 24 h the cast was cut in two longitudinal parts and the glass rod removed. For SEM examination metals were prepared as plates by casting the molten metals on a fireproof glass and then, after solidification, polished using CSi papers and then 6 μm diamond paste.

All reagents were of analytical grade (Prolabo, France). The copper electrodeposition bath was a 1 M $CuSO_4$ + 0.1 M H_2SO_4 solution (bath A), used at 25 °C, and the nickel bath was a 1.42 M $NiSO_4$ +

* Author to whom correspondence should be sent.

0021-891X © 1997 Chapman & Hall

0.33 M $NiCl_2$ + 0.4 M H_3BO_3 solution (bath B), at 45 °C. Voltammetric curves were obtained from nonstirred solutions, at 10 mV s^{-1} which is a usual scan rate to minimize capacitive currents. Deposits were made with various fixed currents, and many T_{pulse}/T_{rest} has been tried from 0.2/2.2 to 2/2.2.

3. Results

3.1. *Electrochemical behaviour of indium, bismuth and InBi alloy in acidic medium*

This study was undertaken to determine the appropriate potential range for electrodeposition of metals without any parasite reaction such as hydrogen evolution. The $E°$ values usually encountered in the literature are −0.581 V vs SCE and −0.041 V vs SCE for the In^{3+}/In and Bi^{3+}/Bi couples [20], respectively.

3.1.1. 0.1 M *H_2SO_4 electrolyte.* The concentration was limited to 0.1 M because higher values destroyed the InBi alloy by preferential dissolution of indium. Typical cyclic voltammetric curves for In, Bi and InBi electrodes are shown in Fig. 1. As In was the major component it was certain that the alloy and pure indium, would have a very similar electrochemical behaviour. Hydrogen evolution started at about −1.3 V vs SCE and oxidization of In to In^{3+} occurred for potentials larger than −0.63 V vs SCE. The presence of In^{3+} in the acid bath was demonstrated by pulse polarography.

Bismuth was oxidized at potentials greater than −0.20 V vs SCE leading to the formation of several adherent oxides (Bi_2O_3, BiO etc). During the reverse cathodic scan the oxides were reduced and proton reduction occurred at −1.2 V vs SCE at the oxide-free metal surface.

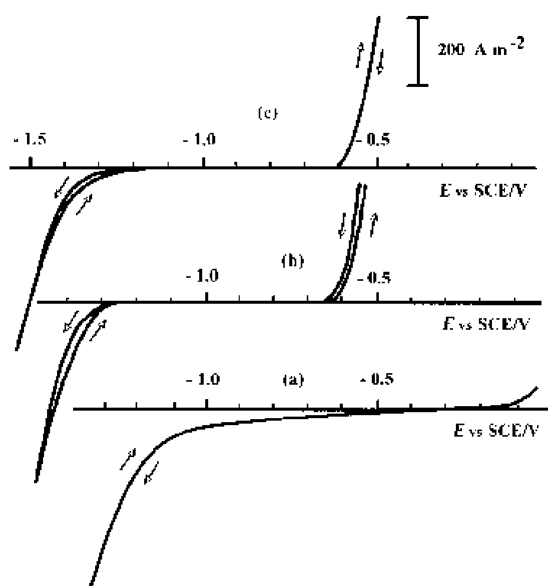

Fig. 1. Electrochemical behaviour of In, Bi, and In–Bi alloy in unstirred 0.1 M H_2SO_4. (a) Bi; (b) In; (c) InBi; electrode area: 0.196×10^{-4} m^2; sweep rate: 10 mV s^{-1}. Scan was started in the cathodic direction from rest potential E_{RP}: (a) -0.53 ± 0.020, (b) -0.65 ± 0.020 and (c) -0.63 ± 0.020 V vs SCE.

3.1.2. 0.4 M *H_3BO_3 + 1.5* M *Na_2SO_4 + 0.66* M *NaCl.* Sodium sulfate and sodium chloride were added to the boric acid in order to obtain the same anion concentrations as in the electrodeposition bath. As shown in Fig. 2 the behaviour of In and InBi were similar. During the anodic scan indium was slightly dissolved for potentials greater than −0.75 V vs SCE and on the next cathodic scan the reduction of In^{3+} ions was observed. Reduction of water started close to −1.4 V vs SCE.

Bismuth was oxidized at about −0.55 V vs SCE and reduction of water was noticeable for potentials lower than –1.6 V vs SCE.

3.2. *Electrodeposition of copper on InBi alloy*

Copper was deposited using bath A. The temperature was fixed at 25 °C and the bath was always vigourously stirred. The cathode area was fixed at 2×10^{-4} m^2 and the copper sheet anode, was 6×10^{-4} m^2.

3.2.1. Rest potential variation of the alloy in the copper bath. Figure 3 shows the potential variation of an In–Bi electrode immersed in the stirred bath. The limiting potential of 0.04 V vs SCE reached after about 3 min was close to that of pure copper in the presence of copper ions.

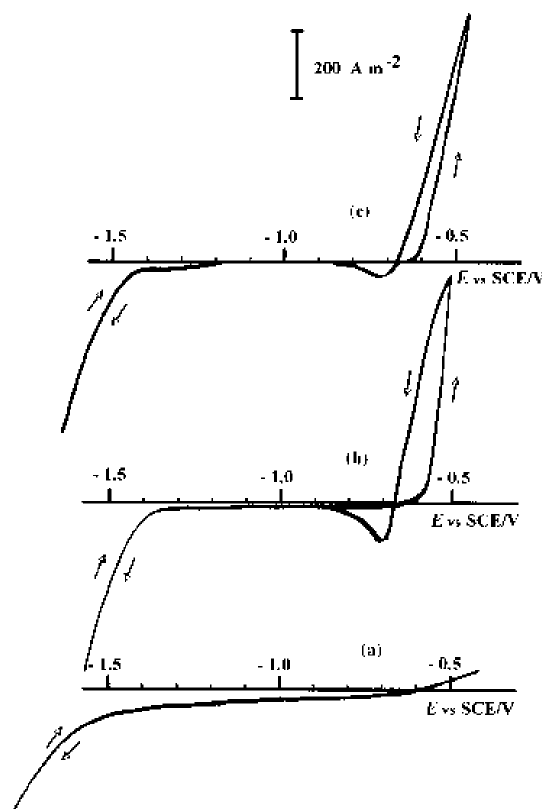

Fig. 2. Electrochemical behaviour of In, Bi and In–Bi alloy in 0.4 M H_3BO_4 + 1.5 M Na_2SO_4 + 0.66 M NaCl. (a) Bi; (b) In; (c) InBi; electrode area: 0.196×10^{-4} m^2; sweep rate:10 mV s^{-1}. The scan was started in the cathodic direction from the rest potential E_{RP}: (a) -0.58 ± 0.020, (b) -0.65 ± 0.020 (c) -0.62 ± 0.020 V vs SCE.

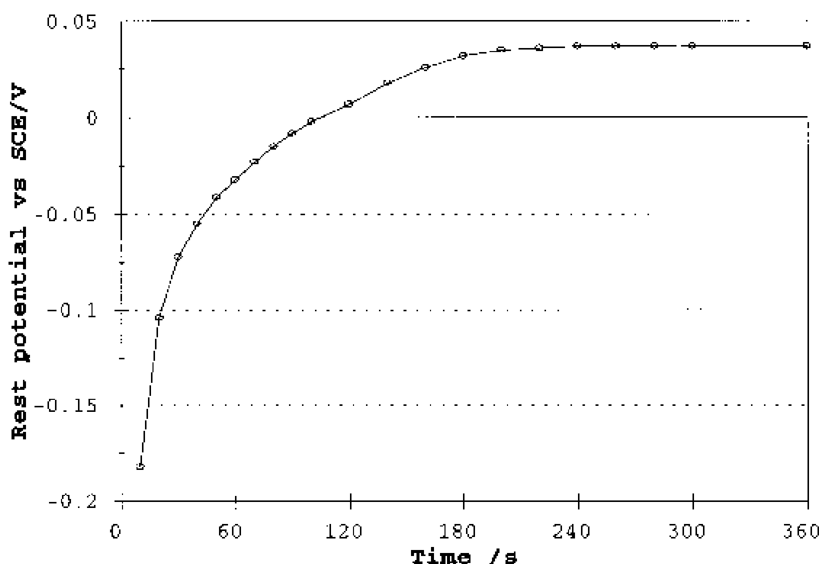

Fig. 3. Variation of the rest potential of In–Bi electrode in 1 M $CuSO_4$ + 0.1 M H_2SO_4 solution.

In the copper solution indium dissolved as follows

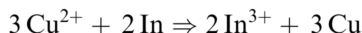

$$3\,Cu^{2+} + 2\,In \Rightarrow 2\,In^{3+} + 3\,Cu$$

After 5 min, a red copper colour was observed at the InBi surface.

3.2.2. Electrochemical behaviour of the alloy in the copper bath. The electrode, initially at −0.35 V vs SCE was progressively made more negative by a cathodic scan. Electrochemical deposition of copper started at potentials lower than –0.56 V vs SCE. During the reverse scan the electrode adopted the behaviour of copper, and the potential where the null current was observed was more anodic (Fig. 4). Then for dissolution, the potential was increased to +0.5 V vs SCE. Several cycles were completed, and because more copper was deposited than dissolved, progressively the electrode behaved like pure copper.

These observations demonstrated that a negative potential had to be applied simultaneously with the immersion when starting the electrodeposition process in order to inhibit the electrochemical cementation phenomenon. As seen in Figure 4 a –0.6 V vs SCE appears to be the upper limit.

3.2.3. Direct current electrodeposition. Table 1 shows data obtained when using selected direct current densities ranging from 500 to 1500 A m^{-2}. In all cases, the deposits were found to be reproducible, adherent, and the electrical yields were always very close to 100%.

Deposits obtained with a current density of 500 to 1000 A m^{-2} were regular and shiny and SEM examination revealed that the grain size was very small. For current densities of 1000 to 1500 A m^{-2} the grain size increased and some irregularities were noticed. Above 1500 A m^{-2}, despite vigorous stirring of the bath, the irregularities became numerous and the deposits exhibited some brown parts. This was a usual phenomenon for copper electrodeposits and it showed a lack of copper ions in the electrode vicinity.

3.2.4. Pulsed current electrodeposition. Usually the T_{pulse}/T_{rest} was less than unity to let the vigorous stirring of the solution renew the electrode vicinity so that at each new pulse the solution appeared to be the same as at the beginning of the deposit. Numerous T_{pulse}/T_{rest} values were tried, from 0.2/2.2 to 2/2.2. No significant differences arised from these values as

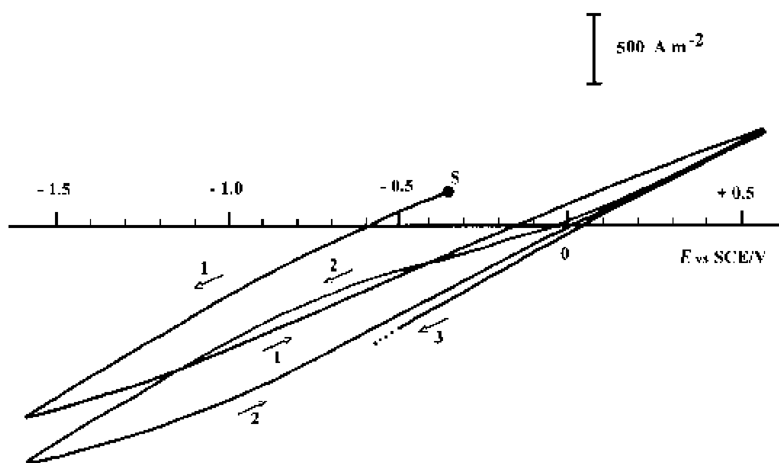

Fig. 4. Typical cyclic curves of In-Bi electrode in unstirred 1 M $CuSO_4$ + 0.1 M H_2SO_4 solution. Electrode area: 0.196×10^{-4} m^2; sweep rate:10 mV s^{-1}.

Table 1. Effect of current density on copper electrodeposition on InBi alloy using direct current

Current density /A m^{-2}	*Deposited mass* / mg	*Cathodic yield* /%	*Anodic yield* /%	*Remaining alloy* / mg
500	117.5	99.2	100	25.2
600	139.5	98.2	99.5	34.4
750	176.8	99.5	100	27.6
850	197.2	98.0	100	30.1
1000	233.8	98.7	99.2	20.0
1250	292.5	98.8	98.8	26.4
1500	351.9	99.0	99.9	24.7

Electrode area: 2×10^{-4} m^2; deposition duration: 3600 s.

regardsthe deposit morphology and current efficiency. Thus, because the aim of the work was to obtain thick deposits, and in order to shorten the rest time and approach the same deposition rate as when using direct current, it was decided to select the duty cycle 2/2.2. The short interruption allowed a periodic return to initial conditions and avoided any defects at the deposit surface.

The electrical yield was always close to 100% (Table 2). It was observed that the upper limit for current density was close to 1250 A m^{-2}, before the quality of the deposit deteriorated.

It may be concluded that pulsed and direct currents produce the same results, probably because the number of instantaneous nuclei on the InBi surface is identical in both cases.

3.2.5. SEM examination of the deposits. During the copper deposition study we noticed that copper could be deposited by cementation without applied current. SEM examination after 0.5 s immersion showed that copper deposits had a skin-like appearance, and did not show any crystallization (Fig. 5). After 20 s immersion the deposits appeared as spherical particles (Fig. 6). There was no evidence for crystallization, because no edges appeared, indicating that cementation was continuing.

When a potential lower than −0.5 V vs SCE was applied to the In–Bi electrode prior to its immersion in the copper bath the deposits were crystallized. The shape of the crystals was identical to deposits ob-

Table 2. Effect of current density on copper electrodeposition on InBi alloy using pulsed current

Current density /A m^{-2}	*Deposited mass* / mg	*Cathodic yield* /%	*Anodic yield* /%	*Remaining alloy* / mg
500	106.9	99.2	100	20.1
600	128.3	99.2	100	22.4
700	151.4	100	100	36.1
850	182.4	99.6	99.8	30.2
1000	215.5	100	100	29.8
1250	268.8	99.8	99.1	32.1
1500	320.3	99.1	99.9	27.8

Electrode area: 2×10^{-4} m^2; $T_{pulse}=2$ s, $T_{rest}=0.2$ s; deposition duration: 3600 s.

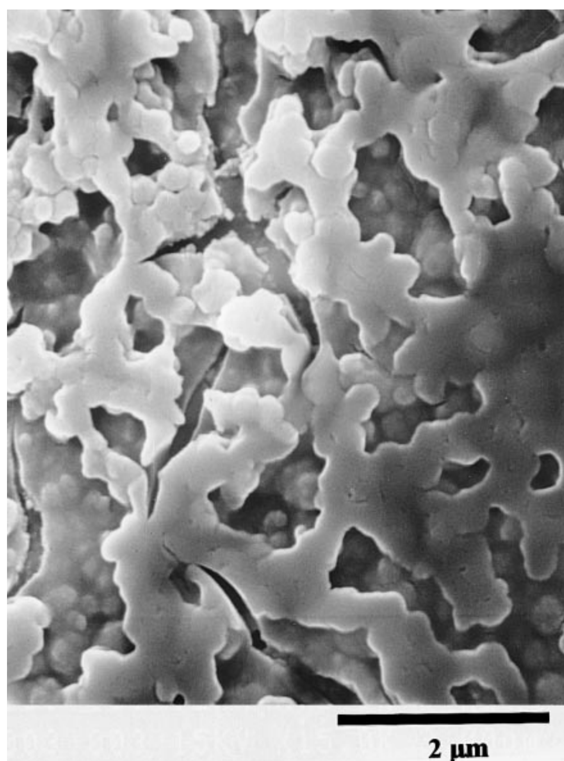

Fig. 5. SEM observation of deposited copper by cementation. Immersion time: 0.5 s in 1 M $CuSO_4$ + 0.1 M H_2SO_4 solution.

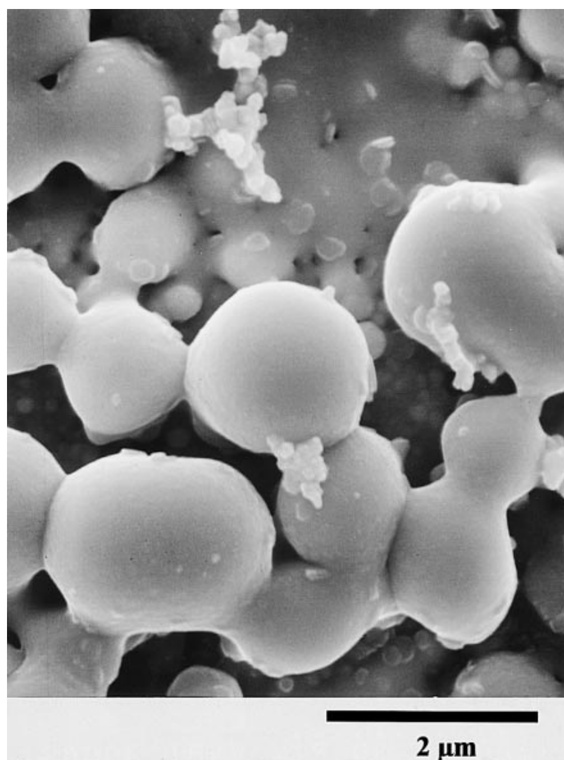

Fig. 6. SEM observation of deposited copper by cementation. Immersion time: 20 s in 1 M $CuSO_4$ + 0.1 M H_2SO_4 solution.

tained by direct (Fig. 7) or periodically interrupted currents (Fig. 8). From these observations it may be concluded that the earlier stages of the electrodeposition did not influence the structure of the thicker deposit, and certainly enhanced the adherence of the deposit compared to the cementation process.

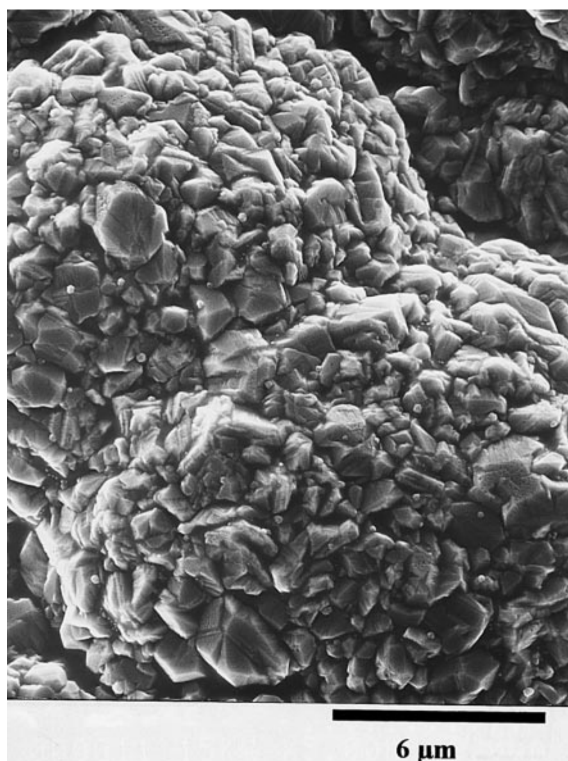

Fig. 7. SEM observation of electrodeposited copper using direct current, in 1 M $CuSO_4$ + 0.1 M H_2SO_4 solution with a current density of 1000 A m^{-2} and a deposition duration of 3600 s.

Fig. 8. SEM observation of electrodeposited copper in 1 M $CuSO_4$ + 0.1 M H_2SO_4 solution under following conditions: duty cycle 2/2.2, current density 1000 A m^{-2} and deposition duration of 3600 s.

3.3. *Electrodeposition of nickel on InBi alloy*

The use of bath B (0.4 M H_3BO_3 + 1.42 M $NiSO_4$ + 0.33 M $NiCl_2$) usually led to good deposits, at a pH of 4.9 and a temperature of 45 °C. The anodes were made of 6×10^{-4} m^2 nickel sheets.

3.3.1. Voltammetry in the nickel bath. The current-potential curves given in Fig. 9 were obtained starting from the rest potential to avoid any indium dissolution. For the two metals and the alloy, it was noticed that the nickel started to deposit at a higher potential compared to that of hydrogen evolution in the bath without nickel (bath B modified, Fig. 2).

3.3.2. Electrodeposition with direct current. Electrodeposition with direct current led to very good deposits for the range 500 to 1250 A m^{-2}. Above this last value, the competition with hydrogen evolution was clearly identified and the deposits became progressively less homogeneous, with more and more cracks. Dissolution of nickel anodes occurred completely, so that the nickel concentration in the bath was kept constant throughout the deposition time.

The electrodeposition was obtained with about a 98% efficiency, provided that the current density remained less than 1250 A m^{-2}. This was found of interest because usually hydrogen evolution was the most important cause for efficiency loss. In the case of InBi, water reduction occurred, as previously shown, only at values more negative than −1.4 V vs SCE, while nickel reduction occurred at −0.9 V vs SCE. So,

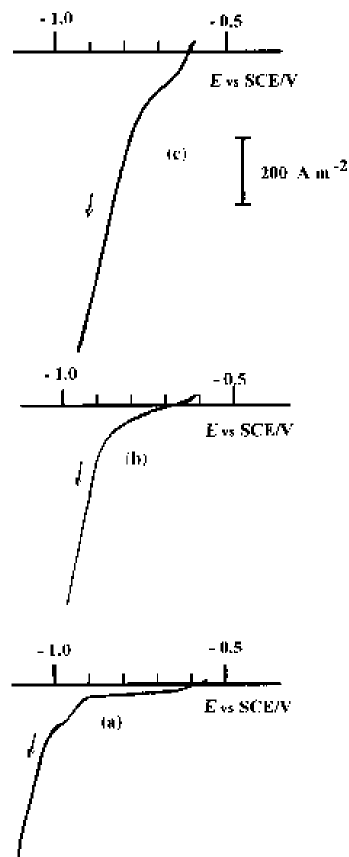

Fig. 9. Typical voltammetric curve of Bi, In and In–Bi in 0.4 M H_3BO_4 + 1.42 M $NiSO_4$ + 0.33 M $NiCl_2$ solution. (a) Bi; (b) In; (c) InBi; electrode area: 0.196×10^{-4} m^2; sweep rate: 10 mV s^{-1}. Scan was started in the cathodic direction from rest potential E_{RP}: (a) -0.58 ± 0.020, (b) -0.65 ± 0.020 and (c) -0.60 ± 0.020 V vs SCE.

at the beginning of the nickel deposition, the water reduction did not occur. As the nickel thickness increased, the water reduction became noticeable but the electrical efficiency was still above 95%. Data are given in Table 3.

Figure 10 shows the variation of the electrode potential during the nickel deposition at several current densities. It was observed that for 500, 700 and 900 A m^{-2} current densities, the potential reached a constant value after about 4 to 5 min.

3.3.3. Pulsed current electrodeposition. A T_{pulse}/T_{rest} ratio ranging from 0.2/2.2 to 2/2.2 was found to have no significant effect on the general morphology of the deposits. In fact, the most influential parameter was the current density. More than 1250 A m^{-2} was to be avoided because the deposits were progressively more rough with several cracks and lacks of nickel due to hydrogen bubbles formation.

Table 4 gives the principal data concerning the deposits.

3.3.4. SEM examination of nickel deposits. The thin nickel deposits of about 3 μm were almost identical when using direct or pulsed currents. A small improvement was seen for pulsed currents where the initial number of nuclei appeared to be larger, leading to a more compact deposit (Figs 11 and 12).

Table 3. Effect of current density on nickel electrodeposition on InBi alloy using direct current

Current density /A m^{-2}	*Deposited mass* /mg	*Cathodic yield* /%	*Anodic yield* /%	*Remaining alloy* /mg
500	107.4	98.0	95.1	19.2
600	127.7	92.6	97.3	49.1
700	148.1	96.6	99.4	34.3
80	170.5	97.3	94.8	20.7
900	194.1	98.5	97.1	19.2
1250	266.5	97.3	95.2	33.5

Electrode area: 2×10^{-4} m^2; deposition duration: 3600 s.

Table 4. Effect of current density on nickel electrodeposition on InBi alloy using pulsed current

Current density /A m^{-2}	*Deposited mass* /mg	*Cathodic yield* /%	*Anodic yield* /%	*Remaining alloy* /mg
500	97.8	98.2	95.0	22.0
750	144.7	97.0	99.0	29.5
1000	199.1	100	99.6	31.2
1250	245.1	98.5	99.8	25.6

Electrode area: 2×10^{-4} m^2; $T_{pulse} = 2$s, $T_{rest} = 0.2$ s; deposition duration: 3600 s.

4. Obtaining the alloy-free copper and nickel shapes

The electrode used for this study was an InBi cylinder of 5.1 mm diameter and 50 mm long. Only 11.5 mm of the tube was immersed in the bath. After electrodeposition the alloy was easily removed from the deposit by heating at a moderate temperature, as the selected InBi alloy has a melting point of 72 °C.

The procedure was as follows: the electrode with the deposit was immersed in hot water ($t = 100$ °C) for complete melting of the alloy. Then the copper or nickel deposit was carefully taken with tweezers, and turned upside down and simultaneously shaken. Using this procedure the major part of the alloy was removed. No optimization of this procedure was undertaken at this time. After separation from the alloy, the deposit was like a pipe, 5 mm in diameter and 11.5 mm in length with one end closed. The amount of alloy remaining on the internal part of the device for either copper or nickel was evaluated by weighing. It was found that the alloy mass remaining after melting ranged from 20 and 35 mg (less than 2% of the total mass). These amounts corresponded to a thickness ranging from 13 to 22 μm, assuming a homogeneous distribution.

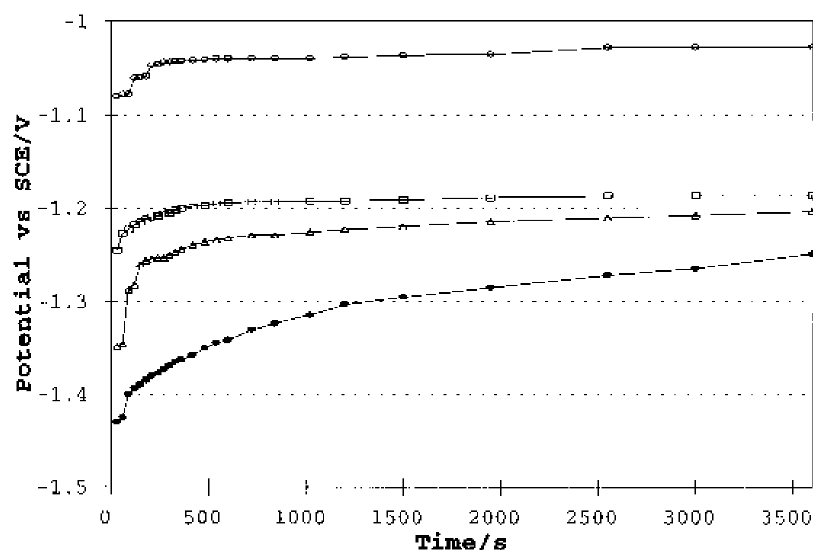

Fig. 10. Variation of the potential during electrodeposition of nickel using direct current, for various current densities: (○) 500, (□) 700, (△) 900 and (●) 1250 A m^{-2}.

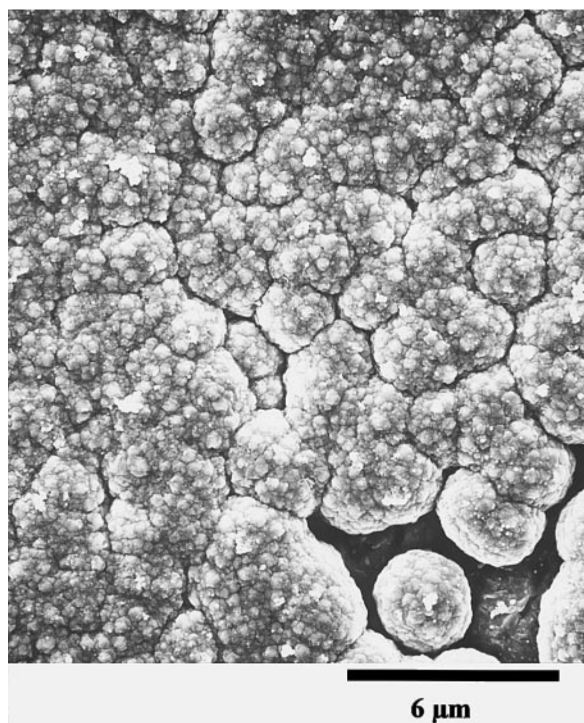

Fig. 11. SEM observation of electrodeposited nickel using direct current, in 0.4 M H_3BO_4 + 1.42 M $NiSO_4$ + 0.33 M $NiCl_2$ solution with a current density of 1000 A m^{-2} and a deposition duration of 3600 s.

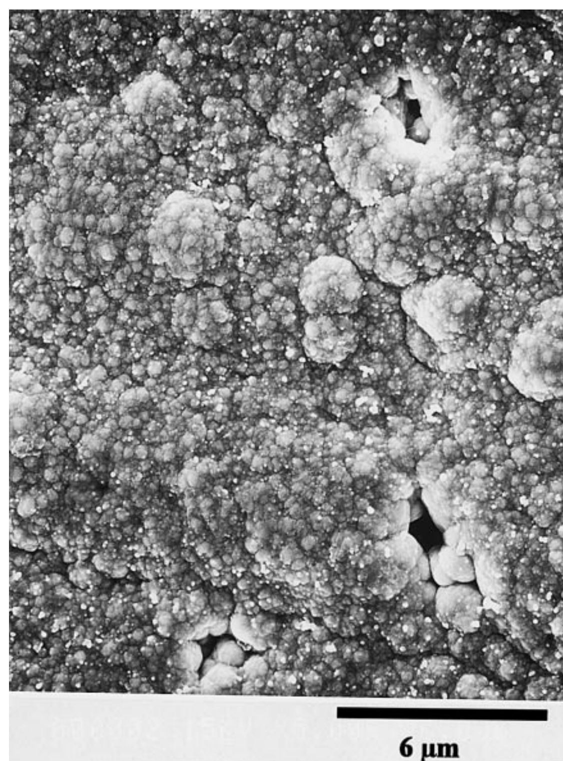

Fig. 12. SEM observation of electrodeposited nickel in 0.4 M H_3BO_4 + 1.42 M $NiSO_4$ + 0.33 M $NiCl_2$ solution under following conditions: duty cycle: 2/2.2, current density: 1000 A m^{-2} and deposition duration: 3600 s.

5. Conclusion

Electrodeposition of copper and nickel on In–Bi electrodes was easily performed using classical baths. Good deposits were obtained, provided the current density did not exceed 1000 A m^{-2}. In both cases, periodically interrupted currents did not lead to better deposits and had no noticeable advantage compared to use of direct currents. The production of special copper or nickel devices was made easier by the use of the 67–33 In–Bi alloy, due to the alloy's low melting point. The ease of the alloy removal allows the manufacturing of small particular devices, for example in jewellery or micromechanics, where normally the machining of such devices would be difficult or time consuming.

References

[1] A. Guntherschulze and H. Betz, *Z. Electrochem.* **37** (1931) 726.
[2] *Idem*, *Z. Phys.* **71** (1931) 106.
[3] L. Masing and L. Young, *Can. J. Chem.* **40** (1962) 903.
[4] A. R. Tourky, T. M. Salem and Z. Hanafi, *J. Chem. U.A.R.* **2** (1967) 131.
[5] I. A. Ammar and M. W. Khalil, *Electrochim. Acta* **16** (1971) 1379.
[6] D. E. Williams, *ibid.* **21** (1976) 1097.
[7] D. E. Williams and G. A. Wright, *ibid.* **21** (1976) 1009.
[8] I. D. Gambury and A. I. Moldov, *Sov. Electrochem.* **27** (1991) 1065.
[9] B. Lovrecek and M. Metikos-Hurovic, *J. Electroanal. Chem.* **106** (1980) 127.
[10] Yu. I. Kuznetsov and S. Yu. Resshetnikov, *ibid.* **27** (1991) 57.
[11] A. S. Bluvshtein, G. N. Mansurov, N. V. Syrchina and O. A. Petrii, *ibid.* **27** (1991) 1182.
[12] T. J. O'keefe and W. Yar-ming, *Corrosion* **41** (1985) 205.
[13] J. Szalema, J. Farkas, L. Kiss, P. Joo and M. Szabo, *Acta Chimica Hungarica* **115** (1984) 53.
[14] G. Budov and V. V. Losev, *Dokl. Akad. Nauk. S.S.S.R.* **129** (1959) 1113.
[15] C. K. Watanabe and K. Nobe, *J. Appl. Electrochem.* **6** (1976) 159.
[16] B. Lovrecek and V. Markovac, *J. Electrochem. Soc.* **109** (1962) 727.
[17] V. Markovac and B. Lovrecek, *J. Electrochem. Soc.* **112** (1965) 520.
[18] G. Serravalle and B. Mazza, *Electrochim. Acta* **8** (1963) 113.
[19] R. Piontelli, G. Poli and G. Serravalle, *Instituto Lambardo* (Rende Sc.) **A93** (1959) 301.
[20] P. W. Atkins, 'Physical Chemistry', W. H. Freeman, New York, 4th edn. (1990).